

## Virtual inline compensation by single point-tracking in free-form bending

SCANDOLA Lorenzo<sup>1,a\*</sup>, BÖHM Viktor<sup>1,b</sup>, MAIER Daniel<sup>1,c</sup> and VOLK Wolfram<sup>1,d</sup>

<sup>1</sup>Chair of Metal Forming and Casting, TUM School of Engineering and Design, Technical University of Munich, Walther-Meissner-Str. 4, 85748 Garching, Germany

<sup>a</sup>lorenzo.scandola@tum.de, <sup>b</sup>viktor.boehm@tum.de, <sup>c</sup>daniel.maier@tum.de, <sup>d</sup>wolfram.volk@tum.de

**Keywords:** Point-Tracking, Process Monitoring, Inline Compensation

**Abstract.** Free-form bending represents an attractive process for the manufacturing of structural components. Due to its kinematics-based working principle, a variety of geometries can be realised in the 3D-space featuring different radii, angles and bending planes. Nevertheless, the kinematic design of the bending head movement represents a complex task, and in order to obtain a part in the desired tolerance range a time-consuming trial and error procedure is the actual state of the art. The part is measured offline and compared to the target geometry after the bending operation, and the analysis of deviations is carried out to derive the compensated bending program. This is not only inefficient, but does not allow for compensating geometrical errors while the process runs. In this paper, a virtual inline compensation strategy based on single point-tracking is proposed. First, the process is modelled virtually and a single point on the component is tracked in space. Subsequently, the obtained tracking signals are presented and explained. Successively a kinematics adaption concept is shown and verified. On a virtual level the results show that the tracking of a single point on the geometry during the process can be used to compensate geometrical deviations in free-form bending.

### Introduction

In the framework of bending processes free-form bending offers a unmatched flexibility regarding the complexity of shapes and geometry that can be obtained. This is of particular interest especially for the automotive sector, where the challenges arising in the e-mobility are setting always more constraints on the design of the chassis to accommodate batteries and additional equipment [1]. In particular concerning the structural components, non-standard parts are required, which can be the result of a lengthy prototypical phase. In such a scenario free-form bending can be the process of choice, as it allows for a fast and relatively low-impact investment manufacturing of components with varying bending features.

The first free-form bending machine has been patented by Murata [2] and belongs to the class of the kinematics-based processes [3]. This confers to the process a virtually infinite freedom of design, as the final geometry is not imposed by the contour of the tool [4]. Independently on the target radius in fact, only a single tool setup is required, designed on the cross-section of the target semi-finished part [5]. This represents a noticeable difference with respect to conventional bending processes, such as rotary-draw-bending [6], which nevertheless introduces a higher complexity in the design of the tool kinematics.

The actual workflow for obtaining a part in the required tolerance range with free-form bending is characterised by a lengthy trial-and-error procedure. In order to react to a deviation from the target geometry, a part must be produced with a trial kinematics, the deviations must be assessed, and basing on this information the new kinematics can be derived. This requires to stop the process and perform an offline measurement of the part, which can eventually lead to long dead times. In order to ensure a robust and defects-free manufacturing of free-form bent parts, an inline

measurement system as well as compensation strategy is clearly identified as the most promising approach, as already demonstrated for other processes such as three-roll push bending [7].

In this study, an inline measurement concept as well as a corresponding compensation strategy is proposed. The investigations are performed virtually on a virtual model of the process, and serve as basis for the future experimental verification of the developed framework. First of all, the digital model of the process is presented and validated, by performing a sensitivity analysis of numerical parameters. Successively, the inline measurement system based on a single point-tracking is described, and the obtained signals are commented. In addition, the sensitivity of the results to the variation of kinematics parameters, such as the target position of the bending head and the feed time, is investigated. Finally, the inline compensation strategy adapting the kinematics based on the inline signals is proposed, and the results are shown.

The investigations aim at showing the feasibility of an inline compensation method for free-form bending, based on a simple and easily implementable inline geometry assessment.

### Virtual representation the free-form bending process

Free-form bending numerical model. The proposed investigations are carried out virtually, making use of a finite element model of the process. The equivalent reduced assembly, consisting of the semi-finished part and of the surfaces of the tools for which contact is established, is shown in Figure 1. The tube is modeled making use of 4-nodes shell elements, featuring reduced integration and hourglass control. In order to reduce the computational time, 5 integration points to the thickness are used, as suggested by Gantner [8]. Due to the small ratio between thickness and diameter,  $t/D \approx 0.06$ , shell elements are preferred over continuum elements. This allows for lower computational time without loss of accuracy. The bending head as well as the fixed holder and the guides are discretised with 4-nodes rigid elements and set up as rigid bodies. The mandrel is composed of 8 balls and a shaft. The elements are connected through MPC with link behaviour [9]. To reproduce the condition of a highly lubricated process the friction coefficient for every contact is set to 0.04 [10]. For the material, the mild steel P235 is taken, and the Young's modulus as well as Poisson's coefficient are set respectively to 210 GPa and 0.3. An experimental flow curve and isotropic hardening are used.

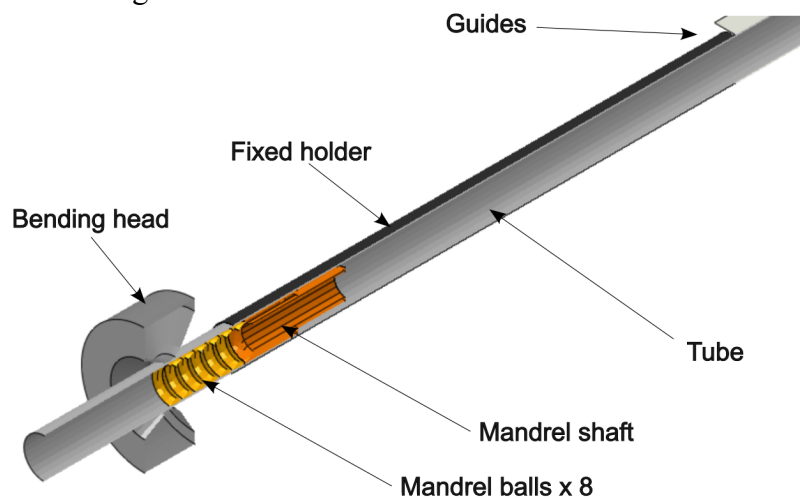


Figure 1: Virtual model of the free-form bending process

Validation of the numerical model. In order to validate the numerical model, different simulations are performed with the aim of assessing the impact on the results. The analysis is performed in Abaqus [11] with the explicit solver. In order to reduce the simulation time, the time scaling strategy is applied. This is preferred over the mass scaling for the free-form bending simulation, as the latter could modify the dynamic behaviour of the part. For this reason, the chosen

numerical parameters for the validation of the model are the time scaling factor and the element size, expressed as number of elements along the tube's circumference. As validation quantity is taken the resulting bending angle. The parameters and results are listed in Table 1.

*Table 1: Investigated parameter sets for the validation of the model*

Time scaling factor	Elements along circumf.	Bending angle in deg
300	30	96.6
190	30	88.4
50	30	87.9
5	30	88.6
190	25	86.6
190	35	86.9
190	40	86.4

The resulting computational times are plotted against the numerical parameters in Figure 2. Regarding the time scaling factor and a fixed number of elements along the circumference of 30, it can be seen that except for the case of very high scaling factors, such as 300, the difference in the bending angle is between 1 *deg*. On the other side, the computational time varies substantially, from about 10 minutes for the case 300 to 14 hours for the case 5. With respect to the number of elements along the circumference with fixed time scaling factor of 190, the angle oscillates around 0.1 *deg*, whereas the resulting computational time also increases exponentially, from 7 minutes for the case of 25 to almost 1.5 hours for the case of 40.

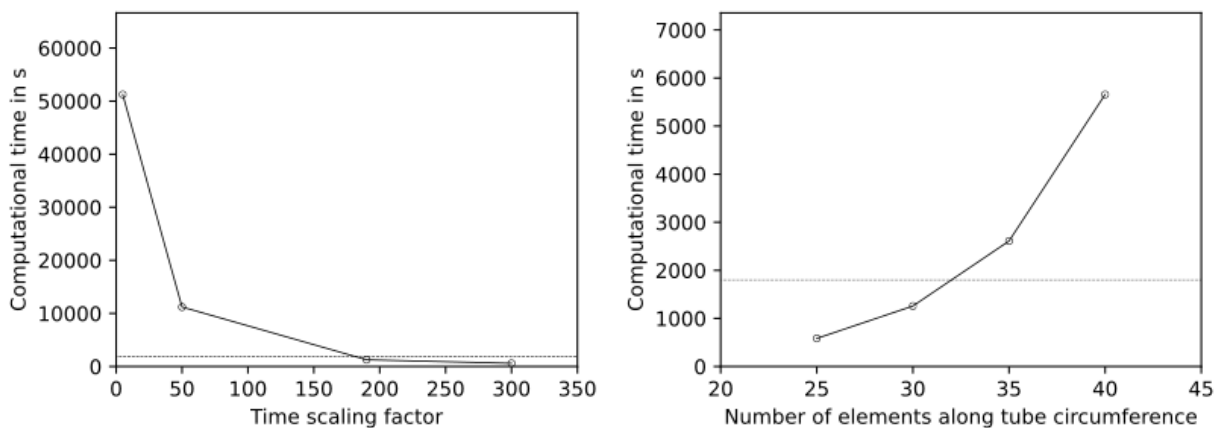


*Figure 2: Elapsed computational time for a free-form bending FEM simulation as a function of the time scaling factor (left) and of the number of elements along the circumference*

For this reason, as standard value for all the following virtual tests, a time scaling factor of 190 and a number of element along the circumference of 30 have been chosen. This allows a computational time lower than 30 minutes, represented as dashed line in Figure 2. Although the results sensitivity to the time scaling is one order of magnitude bigger than that of the mesh size, the benefit in the computational time is such, that the achieved accuracy has been reputed sufficient for the scope of this work. For a more precise simulation, other factors such as the elasticity of the tools, the inertia of the bending head and advanced material modelling for the welding joint and the core material should be addressed.

### Concept of the single point-tracking inline measurement method

Resulting ground signals. The concept for the inline measurement technique is based on the tracking of a single point on the semi-finished part. The tracked point is chosen to be at the starting edge of the tube in the middle of the diameter. The given kinematics of the bending head is shown along with the position of the point during the bending in Figure 3. Four characteristic points can be identified during the bending. The starting configuration can be observed at the time  $t_0$ . From there, the bending head reaches linearly the target position in the time  $t_1$ , where the cantilever beam effect can be observed [12]. Here the constant radius is realised, and this position is held constantly until the time  $t_2$ , where the bending head starts to return to the initial position, which is reached at the time  $t_3$ .

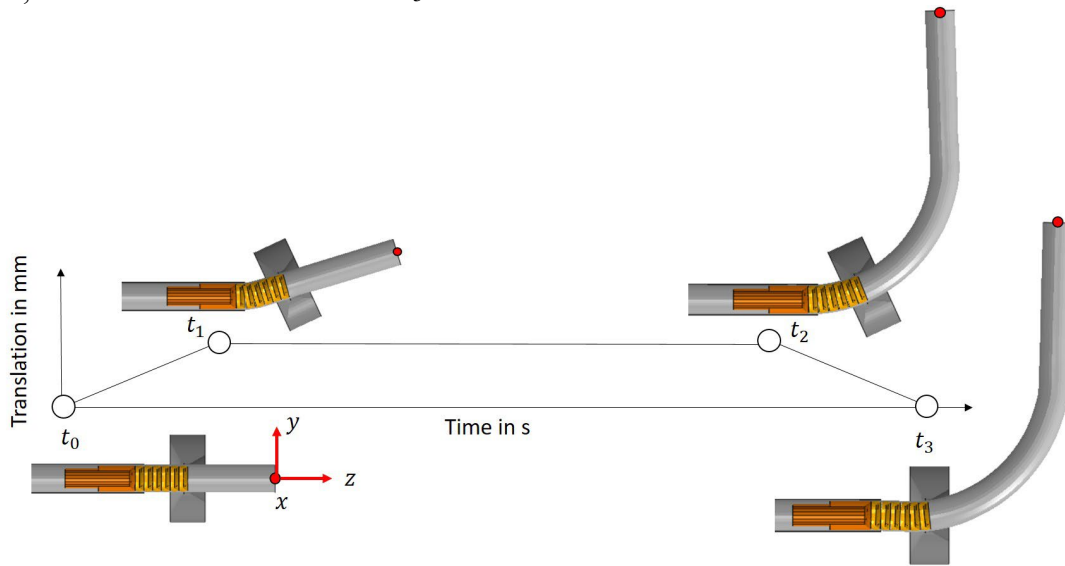


Figure 3: Kinematic path of the bending head and relative position of the tracked point

The inline signals of the tracked point acquired during the process are expressed as the variation of its coordinates during time, with respect to the fixed reference system lying on the point at the beginning of the process, represented in red in Figure 3. These include the  $x$ ,  $y$  and  $z$  coordinates of the point as well as its trajectory, which are shown in Figure 4.

It can be seen, that the  $x$  coordinate (top-right) remains constant as expected and does not yield any information about the bending.

On the other side, the  $y$  coordinate shows an evident bi-linear evolution in time, (top-left). After  $\approx 1$  s the slope of the curve diminishes clearly. This confirms the *cantilever-beam effect* behaviour of the tube at the beginning of the bending [12]. In addition, after reaching a maximum at around  $\approx 5$  s, the  $y$  coordinate of the tracked point decreases, which can be interpreted as a measure of the springback or of an additional bending effect imposed by the bending head to the part when returning to its initial position.

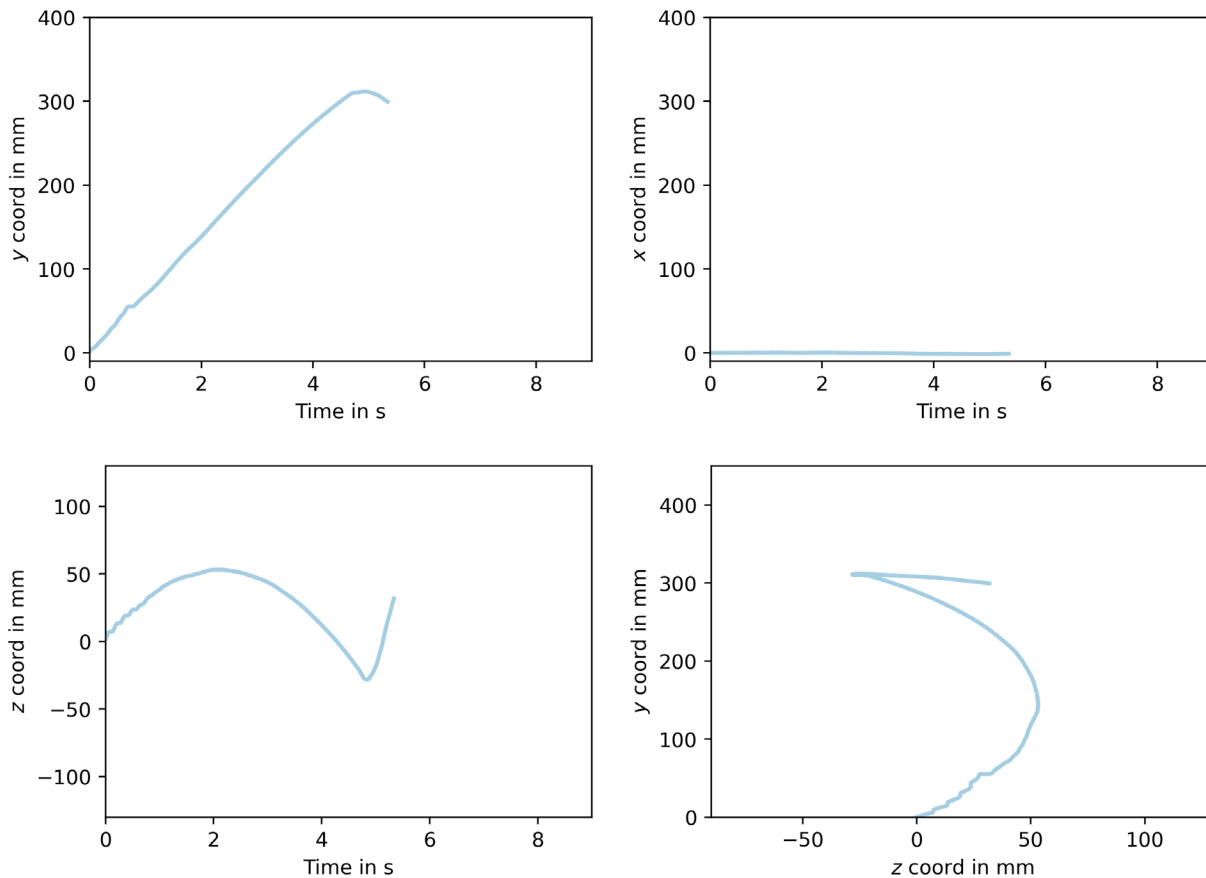


Figure 4: Resulting signals of the tracked point: y coordinate (top-left), x coordinate (top-right), z coordinate (bottom-left), y-z trajectory (bottom-right)

A characteristic signal shape can be also recognised in the z coordinate, (bottom-left). The signal increases first linearly. After reaching a maximum, an inversion in the z coordinate is recorded, since during the bending the tip of the tube is displaced to the opposite direction with respect to the feed. Finally, when the bending head gets back to the initial position the z coordinate increases again.

In addition to the analysis of the evolution of the coordinates of the tracked point in time, its y-z trajectory can also be reconstructed (bottom-right). Again, a clear bi-linear behaviour can be identified when the bending head reaches its target position. Moreover, the final linear decreasing part of the signal can be used as an indication regarding the decrease of the target bending angle.

Sensitivity analysis to variation of kinematics parameters. In order to investigate the sensitivity of the described tracking signals with respect to the free-form bending process, different tests are performed. As kinematics parameters the target position of the bending head  $u$  as well as the total bending time  $t$  are chosen. The tested configurations are summarised in Table 2.

Table 2: Target position and total time configurations for the sensitivity analysis

Label	u 7	u 9	u 11	u 13	u 15	t 3	t 4	t 5	t 6	t 7
Total time $t$ in s	5	5	5	5	5	3	4	5	6	7
Target position $u$ in mm	7	9	11	13	15	11	11	11	11	11

For the interpretation of the results, the final free-form bent geometry is compared to the obtained tracking signals. The former is described using the resulting bending radius and angle,

while for the latter only the  $y$  coordinate is analysed. Although also the  $z$  coordinate and the trajectory yield similar information, see Figure 4, for a 2D-bending in the vertical direction the  $y$  coordinate allows for the simplest data interpretation. The obtained tracking signals of the  $y$  coordinate for different target positions and total time are shown in Figure 5.

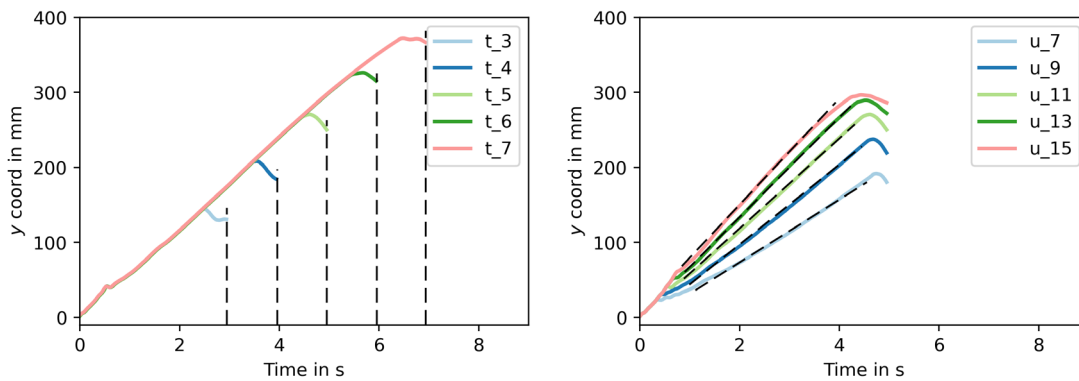


Figure 5:  $Y$  coordinate of the tracked point for different total time (left) and target position (right)

It can be seen that an increase in the total time leads to an increase in the value of the  $y$  coordinate of the tracked point, as it can be recognized in Figure 5 left, where the total time is shown in black dashed lines. In addition, bigger values of the target position of the bending head induce a steeper signal of the  $y$  coordinate, which is represented by the linear fit on the curves in black dashed lines in Figure 5 right. To investigate if the inline signals are suitable to analyse the free-form bending process, the resulting bending parameters are plotted against the inline data in Figure 6.

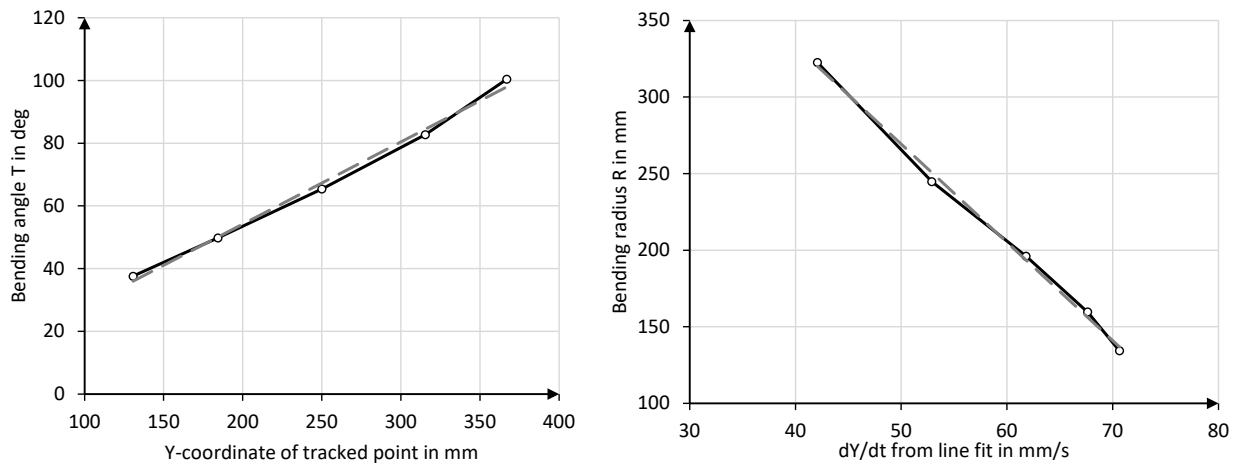


Figure 6: Correlation between inline  $y$  coordinate signal with bending angle (left) and bending radius (right)

The resulting bending angle is shown against the value of the  $y$  coordinate at the end of the bending in Figure 6 left. It can be seen that a linear correlation between the inline signal and the bending angle arises. This is reasonable, since increasing the total time of the bending results in a proportional increase of the achieved angle. The investigations confirm that the phenomenon is linear, with a Pearson Correlation Coefficient of  $R^2=0.994$ .

To investigate the impact of the inline measurement on the obtained bending radius, a line fit is first applied to the linear part of the  $y$  coordinate signals in Figure 5 right (dashed black lines), resulting in the first derivative parameter  $dY/dt$ . Plotting the bending radius against this parameter also yield a linear correlation with  $R^2=0.997$ , shown in Figure 6 right. This means that the slope of

the  $y$  coordinate signal in time correlates linearly with the obtained bending radius, and can hence be used as an indirect measurement of the achieved radius in real time.

The investigations confirmed that the inline tracking of a single point on the bending part can be exploited to assess the values of bending features such as the bending radius and bending angle during the process. This can be used to realise an inline compensation for free-form bent parts.

### Inline compensation strategy

In order to show the potential of the inline tracking measurement for process monitoring and compensation, a starting geometry obtained by a first-guess kinematics, *init* in Figure 7, is used as a starting point to achieve the target geometry, *tgt*. Two approaches are presented, namely the adaption of the process time only, as well as the correction of target position and total time simultaneously.

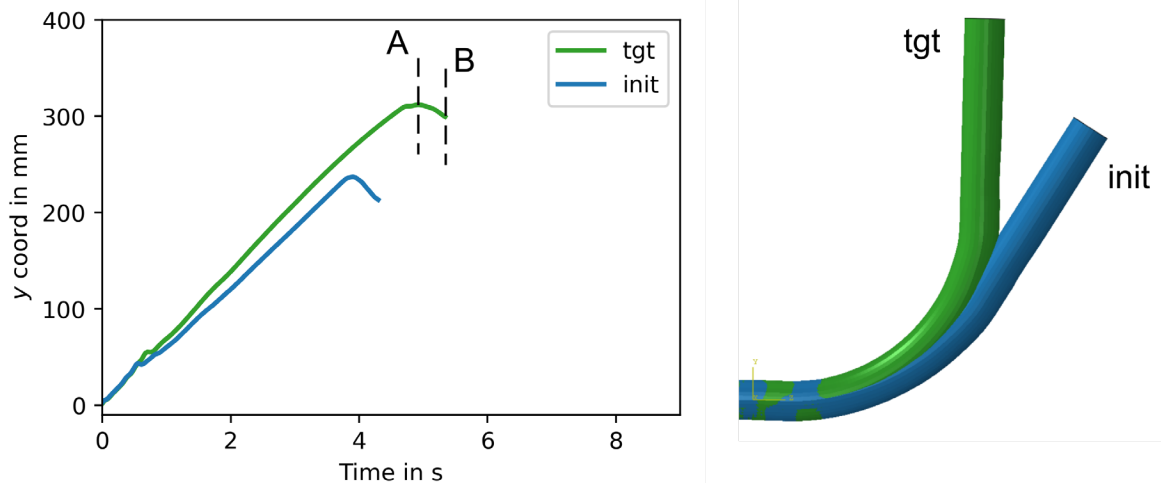


Figure 7: Initial and target  $y$  coordinate tracking signal (left) and resulting geometries (right)

Compensation by time only. The first approach to compensate the part is to modify the total process time only. Since the initial guess results in a much lower bending angle than the target, Figure 7 right, the total time is increased in order to reach a higher angle. In particular, three strategies are tested. In *SIA* the time when the matrix begins to return to the initial position,  $t_2$  in Figure 3, is set as the time where the maximum of the  $y$  coordinate signal of the target part is achieved, *A* in Figure 7 right. On the other hand the kinematics *SIB* is achieved by setting  $t_2$  as the time at which the  $y$  coordinate signal ends, *B* in Figure 7 right. The results are shown in Figure 8, where *SIC* represents the configuration showing the same bending angle as the target, obtained a-posteriori.

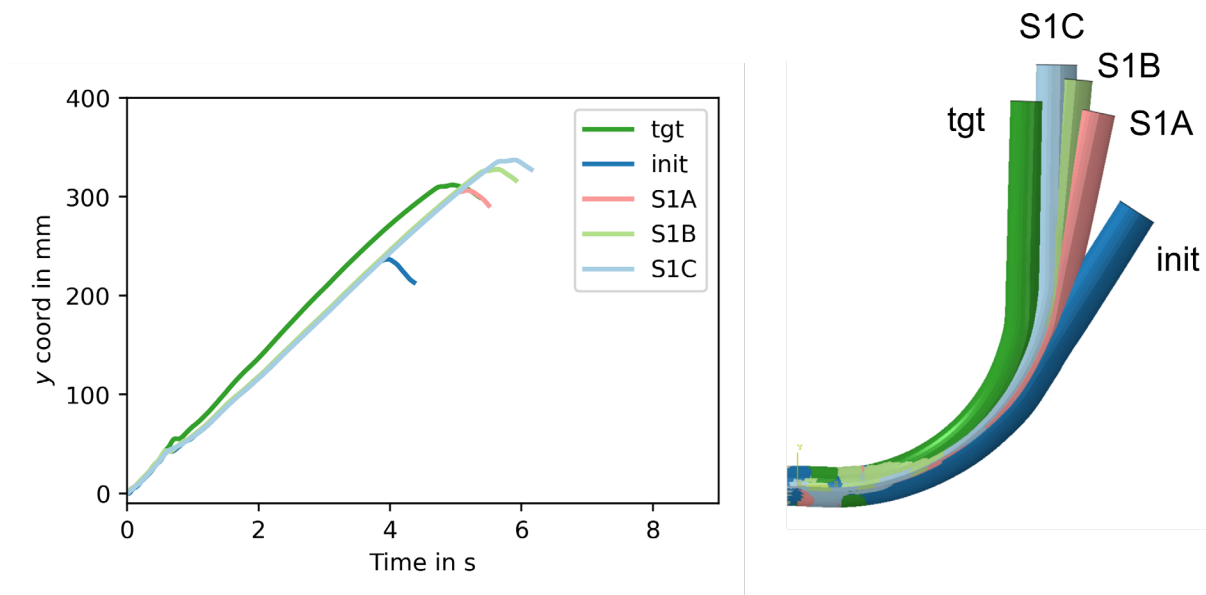


Figure 8: Results of the compensation by adaption of total time: *y* coordinate tracking signals (left) and resulting geometries (right)

It can be observed, that the modification of the total time of the process cannot yield a proper compensated geometry if the target position of the bending head is not correct. This is particularly clear in Figure 8 left. Although the *y* coordinate of *S1A* is very close to the target  $T=88.4\text{ deg}$ , the resulting bending angle is reaching only  $T=78.1\text{ deg}$ . In addition, the closest angle of  $T=88.9\text{ deg}$  can be achieved with the strategy *S1C*, which results in a much higher *y* coordinate. This demonstrates that this method can only be employed successfully when the target bending head position is already correct, and the only geometrical error is represented by the bending angle, making use of linear correlation as shown in Figure 5 left.

Compensation by time and target position. In order to identify the correct kinematics able to yield the target geometry, the inline compensation strategy can be used to first modify the target position of the bending head and then to adapt the total process time. To demonstrate this, two additional kinematics starting from an incorrect target position are tested and modified until the signal of the correct target position is visualised in the *y* coordinate plot. In the kinematic profile *S2inc* the bending head reaches a too little target position, and is further displaced after 0.8 s until the *y* coordinate signal value matches the target *tgt*. The test *S2dec* represents the opposite path, namely the bending head reaching a too high target position, before being displaced to the lower values until the *y* coordinate signals match after 0.8 s. The results are shown in Figure 9, referring to the *y* coordinate signals (left) and the resulting geometries (right). It can be seen that the initial starting geometry could be compensated inline, only comparing the target and obtained tracking signals of a single point. First, the target position of the bending head can be successfully achieved by analyzing the *y* coordinate signal, Figure 9. Both *S2inc*, yellow, and *S2dec*, red, show a *y* coordinate value respectively lower and higher than the target at the beginning, which converge to the target after displacing the bending head in the proper direction. This results in a radius compensation, with a remaining deviation of 12.0 mm for *S2inc* and 1.4 mm for *S2dec*, clearly lower than the one of the initial geometry of 41.3 mm.

At this point, the bending can be held until the actual *y* coordinate signal matches the target one in time, as discussed previously. In such a way, the angle compensation based on the total process time can be carried out, resulting in deviations of 4.4 deg for *S2inc* and 0.01 deg for *S2dec*, and representing a relevant enhancement with respect to the initial geometry deviation of 30.5 deg.



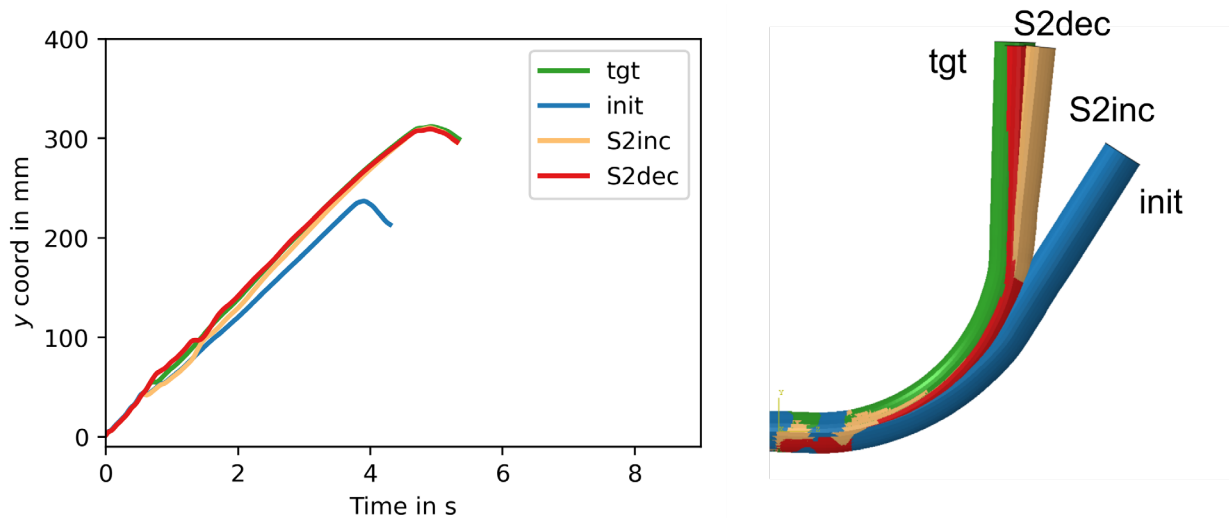


Figure 9: Results of the compensation by adaption of target position and total time: y coordinate tracking signals (left) and resulting geometries (right)

### Conclusions

This paper addressed the topic of inline geometry acquisition and compensation in free-form bending and proposed a novel strategy, based on single point-tracking. The cumbersome trial-and-error approach to obtain parts in the desired tolerance range represents the bottle-neck for the diffusion of the process and is mainly based on offline geometry measurements. Although other approaches, such as inline bending features monitoring and laser tracking have been tested, the problem is still unresolved. In this scenario, the single point-tracking has been developed here and validated by exploiting the virtual model of the process. First, the FE model of the process has been implemented and verified by assessing the impact of the time scaling factor parameter and the mesh size. Successively, the concept of the single point-tracking has been presented, and the ground inline signals referring to the  $y$ ,  $x$ ,  $z$  coordinate as well as the point trajectory have been described. The  $y$  coordinate signal has been chosen as the most representative, and a sensitivity analysis concerning the variation of the total process time and of the target position of the bending head has been performed. The results showed a linear correlation between the bending angle and the absolute  $y$  coordinate value, as well as between the bending radius and the first derivative of the  $y$  coordinate in time, with Pearson coefficients higher than 0.99. Finally, this information has been used to propose an inline compensation strategy. It could be demonstrated, that in order to perform a full geometry compensation both the target position of the bending head as well as the total process time must be adapted. The  $y$  coordinate signal can be used for a 2D-bending to identify the correct value of the target position of bending head, and the total process time can be exploited to correct the angle, provided that the target geometry and associated signals are available. The results allowed to enhance the starting radius and angle deviations of 41.3 mm and 30.5 deg to the values of 1.4 mm and 0.01 deg.

Future work will concern the experimental validation of these investigations, and the comparison with other approaches, such as laser-based geometry acquisitions methods an inline assessment of bending features.

### References

- [1] P. Gantner, H. Bauer, D.K. Harrison, and A.K. de Silva, Free-Bending-A new bending technique in the hydroforming process chain, *J. Mater. Process. Technol.* 167 (2005) 302–308. <https://doi.org/10.1016/j.jmatprotec.2005.05.052>

- [2] M. Murata, Y. Uemura, and H. Suzuki, *Adv. Tech. Plast.* 3 (1990) 1573–1578.  
<https://doi.org/10.1299/kikaic.55.2488>
- [3] DIN Deutsches Institut für Normung e. V., *DIN 8586: Fertigungsverfahren Biegeumformen*, Berlin: Beuth Verlag GmbH (2003)
- [4] J. Neu, 6-Achs Freiformbiegemaschine NSB on <https://www.neu-gmbh.de/de/freiformbiegen-nsb>
- [5] M.K. Werner, L. Scandola, D. Maier, and W. Volk, *Freeform Bending Tool Design for Rectangular Profiles and Its Influence on the Process*, *J. Manuf. Sci. Eng.* 145 (2023).  
<https://doi.org/10.1115/1.4062811>
- [6] B. Engel and M. Hinkel, *Analytisch unterstützte Vorauslegung des Rotationszugbiegeprozesses*, *Tagungsband / XXX. Verformungskundliches Kolloquium: Leoben*, (2011) 97–102
- [7] A. Ghiotti, E. Simonetto, S. Bruschi, and P.F. Bariani, *Springback measurement in three roll push bending process of hollow structural sections*, *CIRP Ann.* 66 (2017) 289–292.  
<https://doi.org/10.1016/j.cirp.2017.04.119>
- [8] P. Gantner, H. Bauer, D. K. Harrison, and A. K. M. de Silva, *FEA - Simulation of Bending Processes with LS-DYNA*, 8th International LS-DYNA Conference (2004)
- [9] X. Guo et al., *Free-bending process characteristics and forming process design of copper tubular components*, *J. Adv. Manuf. Technol.* 96 (2018) 3585–3601.  
<https://doi.org/10.1007/s00170-018-1788-1>
- [10] N. Beulich, P. Craighero and W. Volk, *FEA Simulation of Free-Bending - a Preforming Step in the Hydroforming Process Chain*, *J. Phys. Conf. Ser.* 896 (2017),  
<https://doi.org/10.1088/1742-6596/896/1/012063>
- [11] Dassault Systèmes Simulia Corp, *ABAQUS/Standard User's Manual* (2023)
- [12] L. Scandola, J. Tschannerl, D. Maier, M.K. Werner, C. Hartmann, and W. Volk, *Impact of the process velocities on the quality of free-form bent parts*, *IOP Conf. Ser. Mater. Sci. Eng.*, 1284 (2023). <https://doi.org/10.1088/1757-899x/1284/1/012061>